Precision stress localization during mechanical harvesting of vertically oriented semiconductor micro- and nanostructure arrays

M. M. Ombaba, L. V. Jayaraman, and M. S. Islam

Articles you may be interested in

Microstructure factor and mechanical and electronic properties of hydrogenated amorphous and nanocrystalline silicon thin-films for microelectromechanical systems applications
J. Appl. Phys. 114, 184905 (2013); 10.1063/1.4829020

Controlled growth of vertically oriented molybdenum oxide nanoplates
AIP Conf. Proc. 1536, 35 (2013); 10.1063/1.4810087

GaN epitaxial films grown by hydride vapor phase epitaxy on polycrystalline chemical vapor deposition diamond substrates using surface nanostructuring with TiN or anodic Al oxide
J. Vac. Sci. Technol. B 28, 1011 (2010); 10.1116/1.3488616

Vertically aligned ZnO nanostructures grown on graphene layers
Appl. Phys. Lett. 95, 213101 (2009); 10.1063/1.3266836

Mechanism of nanodiamond film formation by stress relaxation on a preferentially oriented vertical basal plane graphitic precursor
J. Appl. Phys. 89, 5769 (2001); 10.1063/1.1367313

Precision stress localization during mechanical harvesting of vertically oriented semiconductor micro- and nanostructure arrays

M. M. Ombaba, L. V. Jayaraman, and M. S. Islam[a]
Northern California Nanotechnology Center and Electrical and Computer Engineering, University of California, One shields Avenue, Davis, California 95616, USA

A facile protocol of channeling the applied force onto the roots of 1-dimensional (1-d) semiconductor arrays during their mechanical transfer from their mother substrate is presented. This is achieved by fully encasing them in thermally processable matrices with high moduli and impact strength. This approach significantly differs from other complimentary methods as it ensures that the shearing force applied during their transfer is precisely localized at their roots rather than along their full length. The structures remain heterogeneously embedded in the matrix upon transfer, with retention of their pitch, lengths, and integrity. The process is solventless, recycles polystyrene, is rugged, and can potentially be used to transfer a variety of 1-D structures with disregard of their aspect ratio, pitch, and dimensions. We show that millions of micropillars over a large area can be harvested with little sophistication using a hotplate as the only required equipment practically as well as using finite element simulation studies. The protocol is henceforth ripe for high throughput manufacturing. © *2014 AIP Publishing LLC*. [http://dx.doi.org/10.1063/1.4884200]

To date, the exploitation of vertically arranged high aspect ratio one-dimensional (1-D) semiconductor micro- and nanostructures embedded in or atop matrices other than their formative wafers remains a challenge.[1] In part, this is due of lack of an efficient, inexpensive, high fidelity, and throughput platform for rapidly transferring these structures into secondary substrates without compromising their orientation, 3-D spatial distribution, pitch, and mechanically integrity.[1,2] Such a platform could potentially revolutionize the way devices geared towards photovoltaic,[3] thermoelectric,[4] water splitting,[5] optoelectronic,[6] biosensing,[7] and energy storage industries[8] are made and potentially accommodate repetitive structural regeneration and harvesting from a single wafer. This will significantly decrease the cost, bulk, rigidity, and weight of the ensuing devices since the semiconductor wafers are arguably the most expensive, fragile, and heavy component of planar devices.[1,2]

A few protocols of separating vertically arrainged 1-D structures into secondary substrates with preservation of their orientation have been proposed. Notably, Si microwires fully or partially embedded in polydimethylsiloxane (PDMS) can be mechanically cut from the mother wafer with a blade.[9,10] Another complementary approach harvests pre-fractured Si nanowires (NWs) prepared using metal assisted electroless etching (MACE).[11] The transfer-print protocol we have previously explored relies on the ability of structures with certain dimensional criterion to bend and fracture upon application of a lateral force at their tips.[1,2,12] This force correlates to the microwire's spring constant k_s, and its Young's Modulus (E) according to the equation[13]

$$F = k_s = 3\frac{EI}{l^3}s. \tag{1}$$

Although the classical elastic isotropic beam theory indicates that the maximum tensile stress on a 1-D structure under stress should occur at its root, the theory does not preclude the fact that the rest of the structure experiences a significantly high magnitude of stress as it is bound to bend in the direction of the applied force (Fig. 1(a)). Such stress may cause micro and nanocracks along the structures' lengths thus compromise their mechanical integrity. These may be deleterious to their performance in certain device applications. As a matter of fact, these structures have always been found to fracture at points, slightly higher than their interface with the mother substrate especially if their surfaces have defects.[14–16] Given that both bottom up and top down growth techniques bear structures with random defects especially around their roots, they will all fracture at different points, thereby possess statistically distributed lengths.[16] This may hinder repeatable processing and curtail their applications in devices requiring end to end registry due to these stochastic defects.[17]

Therefore, modalities geared towards bend minimization during their transfer could decrease stress along their lengths as well as promote their fracture at precise locations. 2-D finite element simulations indicate that, by encasing the structures with different materials, the stress along the structures can be controlled as the surrounding media could dampen their deflection and movement as illustrated in Fig. 2(b). Materials with high moduli and density like metals stiffen the encased structures, thereby channeling the applied force precisely to their roots as shown in Figs. 2(c) and 2(d). This is beneficial as only a small applied force is needed to cause structural fracture. On the other hand, materials that elastically deform (Poisson ratio (ν) close to 0.5) allow the encased structures to deflect up to some extent (Fig. 2(e)). In addition, the force required to bend or fracture these structures is dependent on their thicknesses. This is illustrated in Fig. 2(f) whereby a log to log plot of the applied force and thickness is indicative of a linear behavior, irrespective of

[a]Author to whom correspondence should be addressed. Electronic mail: Sislam@ucdavis.edu.
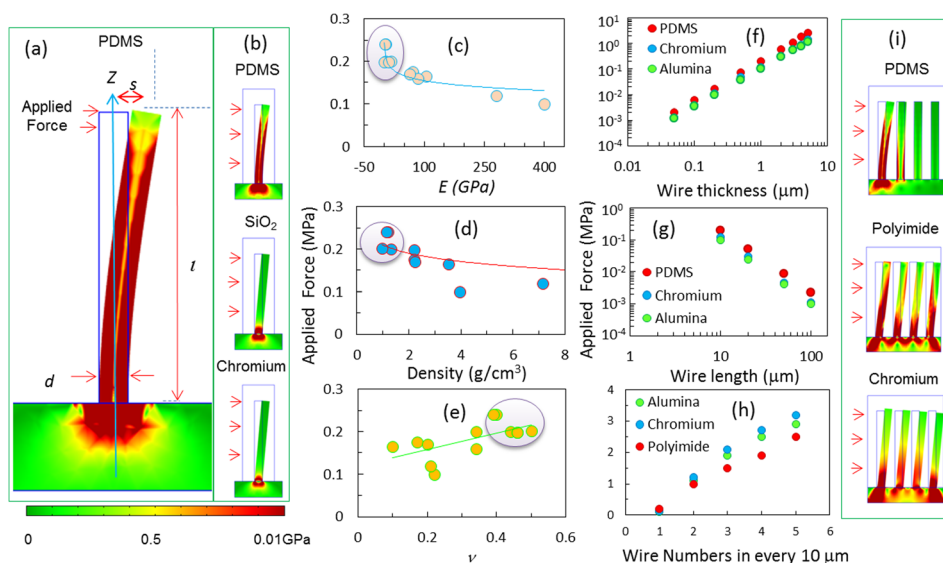
104, 243109-1

FIG. 1. (a) and (b) Finite element 2-D simulation results of a Si microwire atop a Si substrate under stress after application of an appropriate force needed exert a maximum von Misses surface stress of 1 GPa on the Si structure encased in air, PDMS, Silicon dioxide (SiO$_2$), and Chromium. Arrows indicate where the force was applied. Forces required generating a surface stress of at least 1 GPa on the air, PDMS, Chromium, and Alumina encased wires were 15.6, 0.21, 0.12, and 0.1 MPa, respectively. (c)–(e) Exhibits correlations between the Young's Modulus, density, and Poisson ratio of the materials used to encase structures and the respective force needed to exert maximum of a 1 GPa surface stress on the structures. The shaded data points simulated polymeric materials including PMMA, PDMS, polyimide, nylon, and poly(tetrafluoroethylenefluoride). (f)–(h) Effects of structural diameter, length (aspect ratio), and density on the magnitude of the applied force needed to impart at least 1 GPa surface stress on the structures. (i) Surface stress distribution on four wires embedded in PDMS, polyimide, and chromium under stress. Notice that on PDMS, the resultant surface stress is virtually concentrated on the first wire.
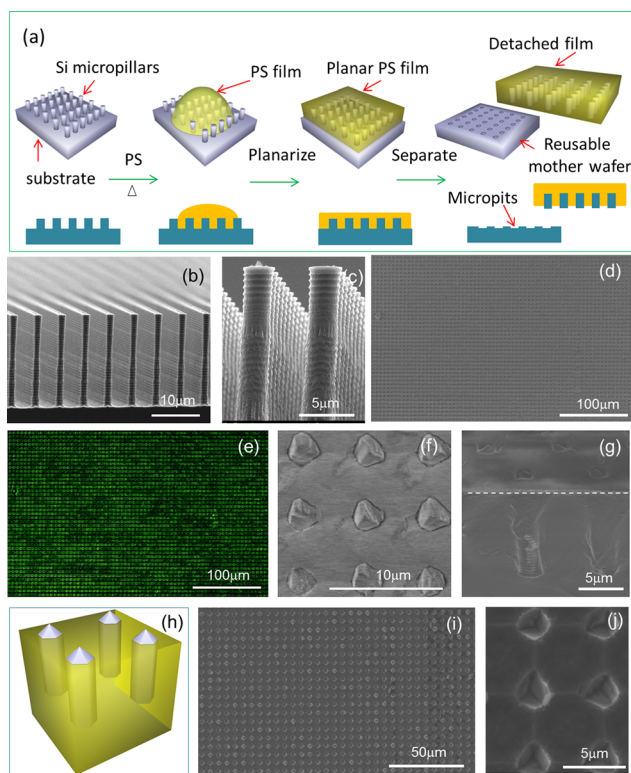

FIG. 2. (a) Steps involved in the uprootal of encased semiconductor micropillars from their mother substrate. SEM images of the micropillar structures. (b) and (c) Before transfer. (d) After transfer and integration into a PS film. (e) Same image enhanced with a neon foreground for clarity. (f) and (g) Higher resolution topographical and cross-sectional images of the integrated film, respectively. (h) Ensuing schematic, depicting the orientation retention of the structures while embedded in PS. Note that the angles of the pillar roots are shown only for clarity and not indicative of the actual crystal planes of the uprooted structures. (i) and (j) SEM of the mother substrate depicting the uniformly sized micropits left micropillar uprootal at low and high magnification.

the structural encasement material. Additionally, one would need to apply a force of a lower magnitude in order to fracture structures with high aspect ratio and vice versa as illustrated in Fig. 2(g). Interestingly though, when structure number/given volume (density) is taken into account, it becomes apparent that one needs to apply more force in order to bend and fracture structures encased in hard materials such as chromium, glass and alumina shown in Fig. 2(h). For example, it would take an applied force of 2.9 and 3.2 MPa to impart a 1 GPa surface stress on 5 microwires, (*diameter* = 1 μm, *length* = 10 μm) encased in the same volume of alumina and chromium compared to 2.5 MPa for those encased in polyimide. On the other hand, although a much smaller force is required to induce a force of similar magnitude on structures embedded on shape deformable materials such as PDMS, the resultant surface stress is mainly concentrated on the first microwire. Additionally, structures encased in polyimide experience a more uniform stress near their roots compared to the former as illustrated in Fig. 2(i). This finding is perhaps the most important discovery of this study as it pinpoints what type of materials should be explored for these kinds of applications. From these preliminary simulation results, it is evident that thermoplastic polymers with high modulus and impact strength could be perfect for structural encasement and transfer as they can be processed at low temperature, distribute the applied force precisely to where it is needed, require less applied force compared to high strength metals and oxides and can be later partially or fully removed to allow for device fabrication by dissolution in a number of solvent.

In this paper, we demonstrate that by encasing semiconductor arrays in polystyrene (PS), their fracturing points during detachment from their mother wafer can be controlled with great precision. This is done by pinning the applied

force precisely to the root of the structures. By so doing, the embedded structures can be detached from their mother substrate in a uniform fashion as illustrated (a). The process is simple. Briefly, the mother wafer was placed on a hot plate that was maintained at 160 °C. A PS piece (used petri-dish) was gently placed atop the structures. The high substrate temperature melted the polymer which subsequently infiltrated and integrated with the structures. A glass slide was placed atop the hot ensemble and a gentle pressure applied to planarize the PS film. Upon cooling, the glass slide was removed and a shearing force applied on the PS film from one side, uniformly uprooting the micropillars from their mother wafer. We used, Si micropillars ($d = 3\ \mu$m, $l = 30\ \mu$m) generated via deep reactive ion etching, whose scanning electron microscopy (SEM) images are depicted in Figs. 3(b) and 3(c). Upon integration with PS and detachment, their SEM micrograph was taken (Fig. 3(d)). Other structures of slightly different diameters underwent a similar facile transfer.[18] The image showcases how large of an array can be detached almost instantaneously using this process. The enhanced micrograph (Fig. 3(e)) better depicts the remarkable uniformity of the integrated array. A close-up of the heterogeneous film (Fig. 3(f)) clearly indicates that the micropillar roots possess striking resemblance, indicative of a uniform uprootal from their mother substrate. Additionally, it was discerned that the micropillars maintained their pitch after transfer. The cross-sectional close-up SEM micrograph of the integrated film (Fig. 3(g)) shows that the micropillars maintained their vertical orientation within the PS matrix. This is better depicted in the ensuing 3-D model (Fig. 3(h)). Similarly, the SEM micrograph of the mother substrate after separation (Fig. 3(i)) depicted uniformly spaced shallow micropits left after array uprootal. Upon observing the substrate under higher magnification (Fig. 3(j)), it became apparent that the heterogeneous film uniformly detached from the mother substrate. This substrate can be further processed and reused to generate more micropillars.
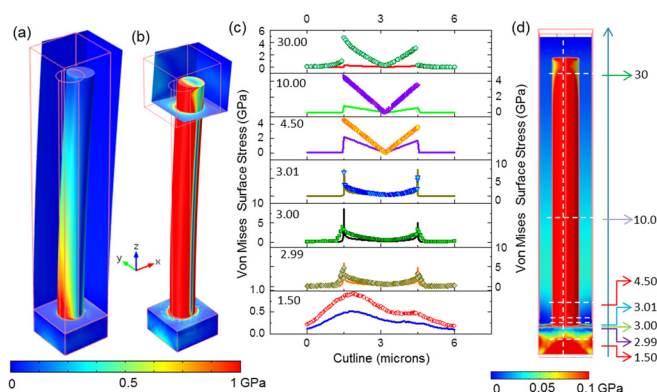
Additional validation of stress localization on structures during transfer was obtained from 3-D simulations using the finite element method (FEM).[18] In the model, a Si microwire ($dia = 1\ \mu$m, $length = 10\ \mu$m) atop a Si wafer was fully (Fig. 3(a)) or partially (Fig. 3(b)) embedded in PS film. A load of 0.01 GPa, way more than what is theoretically[14] required to fracture the single crystalline Si microwire of such dimensions was applied on the PS film in the X-axis. The resultant maximum von Misses surface stress on the fully embedded structure was ~9 GPa and was largely concentrated on its root. On the other hand, it needed 0.02 GPa of load to impart similar stress on the non-embedded structure. Additionally, almost the entire microwire experienced at least 10% of the applied force, consisted with beam bending phenomenon.[19] This was elucidated from the stress force lines on specific points along the ensemble through the middle of the wire in the direction of the applied load as shown in Figs. 3(c) and 3(d). This finding is particularly important as it definitively demonstrates that structural encasement during fracture transfer indeed channels the applied force to structure uprootal. Without encasement, some of the applied force would merely deflect the structures.

Utilization of PS is advantageous over other complimentary polymers as it is inexpensive and widely available. Its low melting temperature (120 °C) and high decomposition temperature (350 °C) compared to other complimentary thermoplastic like PMMA (190 °C and 250 °C, respectively) endows it with a wide thermal window for processability. It can be partially or fully dissolved with common solvents unlike other thermosetting matrices like PDMS that have been used in similar transfers. Its intrinsic high impact resistance and rigidity ensures that it maintains a sturdy stature during the separation. Although other nano/microstructural harvesting modalities such as ultra-sonication[20] and chemical isotropic etching of the roots till they detach do exist,[21] the structures are left in solution, losing their spatial arrangement and orientation. These separation techniques cannot guarantee uniform fracturing points; hence, the harvested structures have dimensional disparities.

Further investigation of the uniformity of the integrated structures was carried out using topographical surface profile lines (Fig. 4(a)) using Gwyddion. These superposed lines possess strikingly similar characteristics (Fig. 4(b)). Their roots slightly protruded from the surface of PS matrix as illustrated (inset therein). Similarly, extracted topographical profile lines of the mother (Fig. 4(d)) exemplified similar observations. The heterogeneous film's low optical transmittance is indicative of its excellent light trapping, amenable for photovoltaic applications (Fig. 4(e)). By beaming a laser light through the heterogeneous substrate at a normal incident angle, a periodic diffraction pattern on a far field screen was obtained (Fig. 4(f)), definitively indicating that the structures preserved their long range pitch and orientation within the PS matrix.[1,11]

The versatility of this transfer process was further extended to harvest Si Nanowires of different diameters grown using chemical vapor deposition as depicted in Fig. 5(a). Here, arbitrary oriented SiNWs as (Figs. 5(b) and 5(c)) readily transferred into PS and remained integrated therein as shown in Figs. 5(d) and 5(e). Ensuing optical transmittance and absorption spectra of the integrated film in

FIG. 3. Simulated von Misses surface stress on a Si microwire fully (a) and partially (b) encased into a PS block upon application of a 0.01 and 0.02 GPa in on the PS block for the former and latter ensemble, respectively, along x-axis. For graphical purposes, a 0–1 GPa surface stress range has been shown to demonstrate that most of the stress on the fully embedded wire is at its root unlike in the latter. (c) Extracted stress lines at specified lengths along the midpoint of the microwires in the x-axis. Maximum stress for the encased structure is at its root (3 μm). Thicker lines depict stress on a bare microwire while thin ones are for the encased structure. (d) The approximate points were the surface stress profiles were collected along the fully embedded structure.
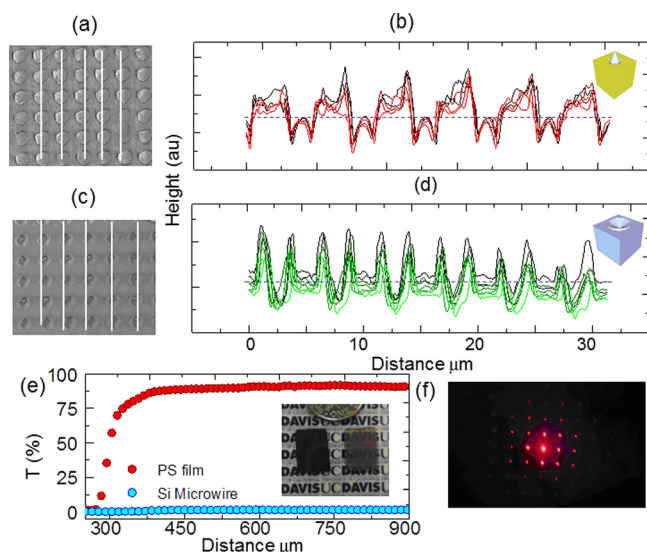
FIG. 4. (a) SEM image of the integrated film depicting topographical lines and the ensuing superposed surface graph (b) exemplifying their remarkable similarity. (c) SEM image of the mother substrate depicting topographical lines used to generate the ensuing superposed surface profiles depicted in (d). (e) Optical transmittance of the integrated film compared to that of PS with similar thickness. (e) Optical diffraction pattern from the HeNe laser beamed through the integrated film at normal incidence on a far field screen.

comparison to a pristine PS film of equal thickness (Figs. 5(f) and 5(g)) demonstrates that the former is highly absorbent across the visible energy band. The deliberately selected rugged mother substrate (inset in Fig. 5(f)) demonstrates that entire arrays can be harvested. Apart from successful transfer of structures in their nano- and microscale, the resultant integrated and mother substrate are largely uniform and defect
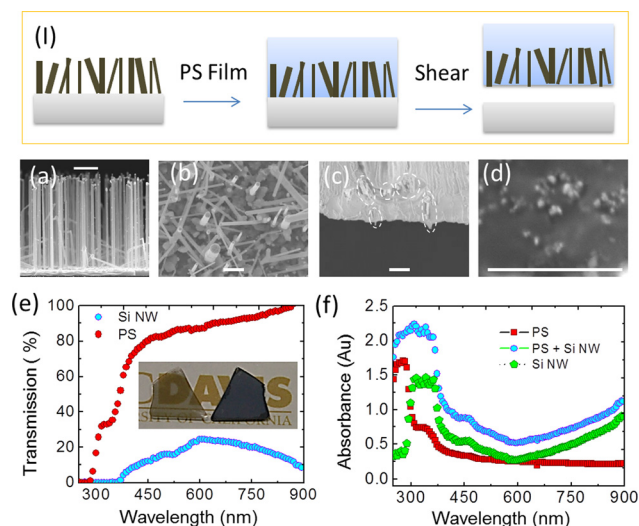

FIG. 5. (a) A depiction of the harvesting processes. (b) and (c) A cross-sectional and topographical SEM image of the SiNWs atop their mother substrate. (d) A cross-sectional view of the integrated film in which SiNWs protruding from and embedded into PS are marked with the dotted line. (e) Topographical image of the integrated film. The light spots are the NW roots embedded into the PS matrix. All scale bars are 2 μm long. (f) Optical transmission spectrum of the integrated film in comparison to PS of equal thickness. Inset is a rugged image of the transferred and integrated structures and their mother substrate. (g) Optical absorption spectra of the integrated film, PS film of equal thickness as well as the subtracted spectrum.

free apart from a few artifacts on some sections of these substrates.[18]

It is true that mechanical harvesting of semiconductor structures from their formative wafers imparts severe stress along their entire length and their fracture is always at random points near their roots. In this communication, the showcased platform amicably addresses these challenges by encasing them into a PS matrix. The platform is adaptable for high throughput manufacturing with minimal sophistication. It is a faster, simpler, rugged, inexpensive, and solvent free alternative to other sophisticated approaches. It could have wide reaching impacts and inspire new interests in emergent research areas that look into effectively harnessing vertically oriented 1-D structures as it enables properties of the transferred structures to be isolated from those of the bulk in an effective way. It is simple, replicable and can perform similar transfers of a variety of structures with disregard of their dimensions and choice of the polymeric matrix.

[1]V. J. Logeeswaran, A. M. Katzenmeyer, and M. S. Islam, IEEE. Trans. Electron Devices **57**, 1856 (2010).

[2]M. M. Ombaba, V. J. Logeeswaran, and M. S. Islam, Appl. Phys. A **111**, 251 (2013).

[3]M. D. Kelzenberg, D. B. Turner-Evans, M. C. Putnam, S. W. Boettcher, R. M. Briggs, J. Y. Baek, N. S. Lewis, and H. A. Atwater, Energy Environ. Sci. **4**, 866 (2011).

[4]J. M. Weisse, A. M. Marconnet, D. R. Kim, P. M. Rao, M. A. Panzer, K. E. Goodson, and X. L. Zheng, Nanoscale Res. Lett. **7**, 554 (2012).

[5]E. A. Santori, J. R. Maiolo, M. J. Bierman, N. C. Strandwitz, M. D. Kelzenberg, B. S. Brunschwig, H. A. Atwater, and N. S. Lewis, Energy Environ. Sci. **5**, 6867 (2012).

[6]W. I. Park, G. F. Zheng, X. C. Jiang, B. Z. Tian, and C. M. Lieber, Nano Lett. **8**, 3004 (2008).

[7]Y. R. Lu, S. M. Peng, D. Luo, and A. Lal, Nat. Commun. **2**, 578 (2011).

[8]A. Vlad, A. L. M. Reddy, A. Ajayan, N. Singh, J. F. Gohy, S. Melinte, and P. M. Ajayan, Proc. Natl. Acad. Sci. U. S. A. **109**, 15168 (2012).

[9]K. E. Plass, M. A. Filler, J. M. Spurgeon, B. M. Kayes, S. Maldonado, B. S. Brunschwig, H. A. Atwater, and N. S. Lewis, Adv. Mater. **21**, 325 (2009).

[10]K. Seo, M. Wober, P. Steinvurzel, E. Schonbrun, Y. Dan, T. Ellenbogen, and K. B. Crozier, Nano Lett. **11**, 1851 (2011).

[11]J. M. Weisse, D. R. Kim, C. H. Lee, and X. Zheng, Nano Lett. **11**, 1300 (2011).

[12]V. J. Logeeswaran, J. Oh, A. P. Nayak, A. M. Katzenmeyer, K. H. Gilchrist, S. Grego, N. P. Kobayashi, S. Y. Wang, A. A. Talin, N. K. Dhar, and M. S. Islam, IEEE J. Sel. Top. Quantum Electron. **17**, 1002 (2011).

[13]W. C. Young, *Roark's Formulas for Stress and Strain* (McGraw-Hill, New York, 1989).

[14]T. Namazu, Y. Isono, and T. Tanaka, J. Microelectromech. Syst. **9**, 450 (2000).

[15]S. Hoffmann, I. Utke, B. Moser, J. Michler, S. H. Christiansen, V. Schmidt, S. Senz, P. Werner, U. Gösele, and C. Ballif, Nano Lett. **6**, 622 (2006).

[16]F. M. Ross, J. Tersoff, and M. C. Reuter, Phys. Rev. Lett. **95**, 146104 (2005).

[17]J. H. Ahn, H. S. Kim, K. J. Lee, S. Jeon, S. J. Kang, Y. Sun, R. G. Nuzzo, and J. A. Rogers, Science **314**, 1754 (2006).

[18]See supplementary material at http://dx.doi.org/10.1063/1.4884200 for 3-D FEM simulation setup, extra SEMs, and artifact analysis.

[19]P. M. Wu, N. Anttu, H. Q. Xu, L. Samuelson, and M. E. Pistol, Nano Lett. **12**(4), 1990 (2012).

[20]W. L. Xu, V. Palshin, and J. C. Flake, J. Electrochem. Soc. **156**, H544 (2009).

[21]S. S. Yoon and D. Y. Khang, Small **9**, 905 (2013).